

FIG. 2. Experimental observation of the 21,0–17,1 vibration–rotation transition of  $\text{HD}^+$ . The nuclear hyperfine level structure and strongest transitions are shown above the observed spectrum.

change in the hyperfine constants, the deuteron contact interaction increasing markedly, with a corresponding decrease in the proton interaction (see Fig. 2); the above coupling scheme is not now appropriate, so that the  $\Delta G_1 = \pm 1$  transitions have intensities comparable to those with  $\Delta G_1 = 0$ . A complex hyperfine pattern is observed, and our spectrum (obtained in an 8 h scan) is shown in Fig. 2, with an unambiguous assignment of the lines. The vibration–rotation frequency is  $984.331 \text{ cm}^{-1}$ .

The simplest approach to the quantitative analysis of the spectrum is to consider only the Fermi contact interactions; we then obtain the following hyperfine constants (in MHz):

$$v = 17, N = 1: b_{\text{H}} = 708, b_{\text{D}} = 113$$

$$v = 21, N = 0: b_{\text{H}} = 134, b_{\text{D}} = 196.$$

Division by the appropriate free-atom hyperfine constants reveals that there is a small asymmetry in the electron distribution for  $v = 17$ , but a very large asymmetry for  $v = 21$ ; the vibrationally averaged electron density at the proton is 0.094, and at the deuteron 0.902. The molecule may be regarded as a deuterium atom interacting weakly with a proton at long range.

Wolniewicz and Poll<sup>1</sup> predict that the last bound level (21,3) lies only  $1.82 \text{ cm}^{-1}$  below dissociation and we shall now search for transitions to this level. Calculations of the vibration–rotation levels based upon the Born–Oppenheimer potential of Peek<sup>3</sup> give a moderately good account of the energies, but the huge asymmetry in the electron density distribution observed in this work is, of course, totally inconsistent with the Born–Oppenheimer approximation.

A. C. thanks the Royal Society for a Research Professorship. We also thank B.P. for a Research Studentship to C.A.M. and the S.E.R.C. for a Research Studentship to I.R.M. and grants towards the purchase of apparatus.

<sup>1</sup>L. Wolniewicz and J. D. Poll, *Mol. Phys.* **59**, 953 (1986).

<sup>2</sup>A. Carrington and J. Buttenshaw, *Mol. Phys.* **44**, 267 (1981); A. Carrington, J. Buttenshaw, and R. A. Kennedy, *Mol. Phys.* **48**, 775 (1983); A. Carrington and R. A. Kennedy, *Mol. Phys.* **56**, 953 (1985).

<sup>3</sup>J. M. Peek, *J. Chem. Phys.* **43**, 3004 (1965).

## Alignment and orientation of $\text{N}_2$ scattered from $\text{Ag}(111)$

Greg O. Sitz, Andrew C. Kummel, and Richard N. Zare

*Department of Chemistry, Stanford University, Stanford, California 94305*

(Received 14 May 1987; accepted 26 June 1987)

When an atom or molecule scatters from a surface, the forces acting during the encounter are not isotropic; instead they possess directionality which manifests itself in the velocity and angular distribution of the scattered particles<sup>1</sup> as well as in the spatial distribution of the angular momentum vectors.<sup>2</sup> This last feature is conveniently expressed in terms of the multipole moments of the distribution in which the odd moments describe orientation and the even moments alignment.<sup>3</sup> This letter reports the measurement of the alignment and orientation of  $\text{N}_2$  scattered from  $\text{Ag}(111)$ , specifically, the quadrupole moment  $A_0^{(2)}(J) = \langle (3J_z^2 - J^2)/J^2 \rangle$ , the hexadecapole moment,  $A_0^{(4)}(J) = \langle (3J^4 - 6J^2 - 30J_z^2J^2 + 25J_z^4 + 35J_z^2/8J^4) \rangle$ , the dipole moment

$A_{-1}^{(1)}(J) = \langle J_y/J \rangle$ , and an octopole moment  $A_{-1}^{(3)}(J) = (3/8)^{1/2} \langle (J_y(5J_z^2 - J^2 + 5J_z + 2)/J^3) \rangle$ , where  $\mathbf{J}$  is the angular momentum operator,  $y$  lies along the laser propagation direction, and  $z$  lies along the surface normal.

A pulsed supersonic beam of  $\text{N}_2$  seeded in He or  $\text{H}_2$  is directed at a clean  $\text{Ag}(111)$  crystal which is held in an UHV chamber ( $4 \times 10^{-10}$  Torr).<sup>4,5</sup> The beam has a rotational temperature of  $\sim 5$  K and is incident along the [211] azimuth. The scattered  $\text{N}_2$  is detected by two-photon resonant, four-photon ionization.<sup>6,7</sup> The ions are detected in a time-of-flight mass spectrometer.<sup>5</sup> The laser beam propagates perpendicular to the plane defined by the molecular beam and the surface normal. To determine the degree of polarization

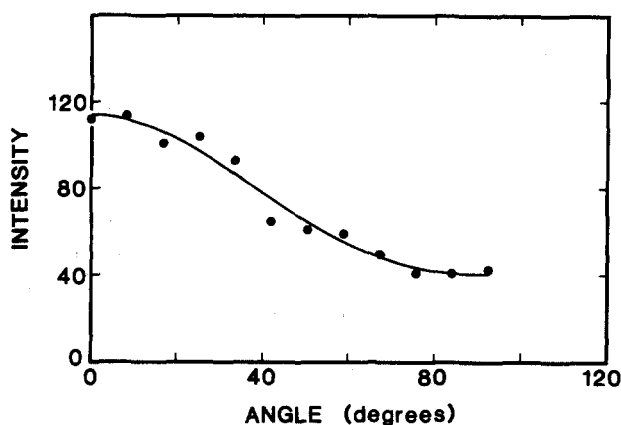


FIG. 1. Variation of the integrated ion intensity with laser polarization angle for linearly polarized excitation of  $O(14)$  for  $N_2$  scattered from  $Ag(111)$ . The angle is measured with respect to the surface normal. The experimental conditions were incident translational energy  $E_i = 0.2$  eV, incident angle  $\theta_i = 15^\circ$ , exit angle  $\theta_f = 20^\circ$ , and surface temperature  $T_s = 390$  K. The solid curve is a least-squares fit which yields  $A_0^{(2)}(J = 14) = -0.92 \pm 0.11$  and  $A_0^{(4)}(J = 14) = +0.37 \pm 0.18$ .

of a particular rotational state of the scattered  $N_2$ , the intensity of a transition originating from the desired level is measured while the laser polarization is varied.

The measurement of the alignment moments  $A_0^{(2)}(J)$  and  $A_0^{(4)}(J)$  is accomplished by rotating the plane of polarization of the linearly polarized laser (by means of a double Fresnel rhomb or a half-wave plate) with respect to the surface normal. An example of this type of measurement is shown in Fig. 1 for the  $J = 14$  line of the  $O$  branch. The solid circles are the data points, and the curve is a least-squares fit yielding  $A_0^{(2)}(J = 14) = -0.92 \pm 0.11$  and  $A_0^{(4)}(J = 14) = +0.37 \pm 0.18$ . A complete description is given elsewhere<sup>7,8</sup> of the determination of  $A_0^{(2)}(J)$  and  $A_0^{(4)}(J)$  from data such as Fig. 1.

The orientation moments  $A_{-1}^{(1)}$  and  $A_{-1}^{(3)}$  are determined as follows. We record the intensity of a particular transition while varying the degree of ellipticity of the polarized light by rotating a half-wave plate in front of a fixed-quarter wave plate, the optic axis of which is positioned along the surface normal. An example of the data is shown in Fig. 2(a) for the  $O(14)$  line, and in Fig. 2(b) for the  $P(14)$  line. The abscissa is read as follows:  $\beta = 0^\circ$  corresponds to linear polarization,  $\beta = \pm 45^\circ$  to left or right circular polarization, and intermediate  $\beta$  values are elliptical polarization where the major axis of the ellipse is the optic axis of the quarter-wave plate. The difference between  $+\beta$  and  $-\beta$  is only in the sense of rotation of the electric field vector. The solid curves represent a least-squares fit to the data from both branches, yielding  $|A_{-1}^{(1)}(J = 14)| = 0.25 \pm 0.02$  and  $|A_{-1}^{(3)}(J = 14)| = 0.15 \pm 0.05$ . Measurements at an incident and final angle of  $0^\circ$ , i.e., along the surface normal, show no asymmetry about  $\beta = 0^\circ$  as would be expected since symmetry dictates that there can be alignment but no net orientation at this angle. We find the degree of orientation to vary

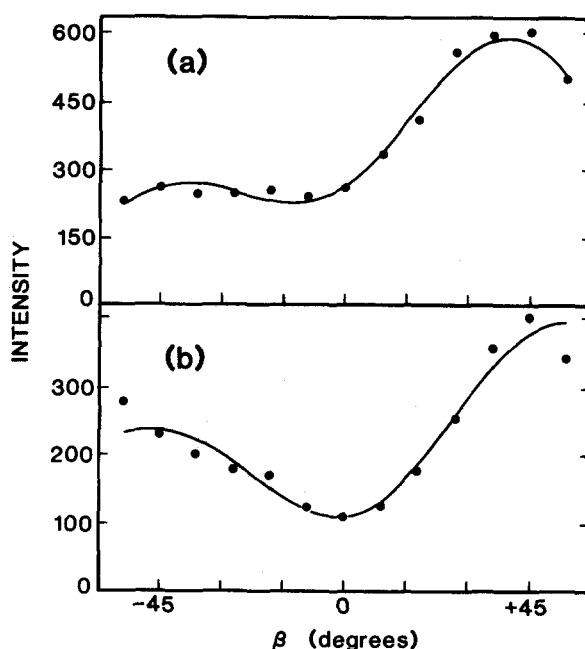


FIG. 2. Variation of the integrated ion intensity vs laser polarization ellipticity for  $E_i = 0.3$  eV,  $\theta_i = 30^\circ$ ,  $\theta_f = 30^\circ$ , and  $T_s = 90$  K (a) for  $O(14)$  and (b) for  $P(14)$  excitation. The solid curves are the result of a least-squares fit to the data in both branches yielding  $|A_{-1}^{(1)}(J = 14)| = 0.25 \pm 0.02$  and  $|A_{-1}^{(3)}(J = 14)| = 0.15 \pm 0.05$ . The signs of  $A_{-1}^{(1)}$  and  $A_{-1}^{(3)}$  are opposite.

strongly with  $J$ , with initial and final scattering angle, and with surface temperature. These results, as well as a complete discussion of the determination of the  $A_{-1}^{(1)}(J)$  and  $A_{-1}^{(3)}(J)$  moments, will be presented in a future publication.<sup>9</sup> The observation of a nonzero value for the orientation moments indicates that there is a propensity for clockwise or counterclockwise rotation of the scattered  $N_2$  when viewed with respect to the laser propagation direction. The sign of the  $A_{-1}^{(1)}(J)$  and  $A_{-1}^{(3)}(J)$  moments is currently being investigated; however, we find these terms always to be opposite in sign.

The alignment has been measured as a function of  $J$  and is found to be more pronounced with increasing rotational excitation, approaching the limiting values for  $J$  being at right angles to the surface normal for large  $J$ .<sup>7</sup> This result indicates that the scattered  $N_2$  is very highly aligned and agrees with the predictions of various models involving the collision of a rotor with a flat or weakly corrugated surface.<sup>10-15</sup> The alignment is found to vary slightly with surface temperature, incident and exit scattering angle, or incident energy.

The degree of orientation is clearly nonzero, but is less than its limiting value of  $A_{-1}^{(1)}(J) = \pm 1.0$ . The observation of a net orientation (or helicity) of the scattered molecules indicates that there are in-plane forces acting during the collision. This conclusion cannot be accounted for in modeling the collision as a rigid rotor with a flat surface, but implies the existence of surface corrugation and/or surface friction. If the observed orientation is due to corrugation of the gas-surface potential, then this type of measurement is seen to be very sensitive, since the corrugation of the closed-packed

face of metal surfaces, particularly silver, is known for He and H<sub>2</sub> diffraction to be very small.<sup>16</sup>

We wish to thank Melissa A. Hines for valuable assistance, and to acknowledge the financial support of the Office of Naval Research under Contract No. N00014-87-K-0265.

<sup>1</sup>J. A. Barker and D. J. Auerbach, *Surf. Sci. Rep.* **4**, 1 (1984).

<sup>2</sup>A. W. Kleyn, A. C. Luntz, and D. J. Auerbach, *Phys. Rev. Lett.* **47**, 1169 (1981); *Surf. Sci.* **152/153**, 99 (1985).

<sup>3</sup>K. Blum, *Density Matrix Theory and Applications* (Plenum, New York, 1981).

<sup>4</sup>G. D. Kubiak, J. E. Hurst, H. G. Rennagel, G. M. McClelland, and R. N. Zare, *J. Chem. Phys.* **79**, 5163 (1983).

<sup>5</sup>G. D. Kubiak, G. O. Sitz, and R. N. Zare, *J. Chem. Phys.* **83**, 2538 (1985).

<sup>6</sup>K. L. Carleton, K. H. Welge, and S. R. Leone, *Chem. Phys. Lett.* **115**, 492 (1985); N. van Veen, P. Brewer, P. Das, and R. Bersohn, *J. Chem. Phys.* **77**, 4326 (1982).

<sup>7</sup>G. O. Sitz, A. C. Kummel, and R. N. Zare, *J. Vac. Sci. Technol. A* **5**, 513 (1987).

<sup>8</sup>A. C. Kummel, G. O. Sitz, and R. N. Zare, *J. Chem. Phys.* **85**, 6874 (1986).

<sup>9</sup>A. C. Kummel, G. O. Sitz, and R. N. Zare (in preparation).

<sup>10</sup>C. W. Mulhausen, J. A. Serri, J. C. Tully, G. E. Becker, and M. J. Cardillo, *Isr. J. Chem.* **22**, 315 (1982); C. W. Mulhausen, L. R. Williams, and J. C. Tully, *J. Chem. Phys.* **83**, 2594 (1985).

<sup>11</sup>J. A. Barker, A. W. Klyne, and D. J. Auerbach, *Chem. Phys. Lett.* **97**, 9 (1983).

<sup>12</sup>J. G. Lauderdale, J. F. McNutt, and C. W. McCurdy, *Chem. Phys. Lett.* **107**, 43 (1984).

<sup>13</sup>R. J. Wolf, D. C. Collins, Jr., and H. R. Mayne, *Chem. Phys. Lett.* **119**, 533 (1985); C. Y. Kuan, H. R. Mayne, and R. J. Wolf, *ibid.* **133**, 415 (1987).

<sup>14</sup>T. R. Proctor, D. J. Kouri, and R. B. Gerber, *J. Chem. Phys.* **80**, 3845 (1984).

<sup>15</sup>G. C. Corey and M. H. Alexander, *J. Chem. Phys.* (submitted).

<sup>16</sup>J. M. Horne and D. R. Miller, *Surf. Sci.* **66**, 365 (1977); J. M. Horne, S. C. Yerkes, and D. R. Miller, *ibid.* **93**, 47 (1980).

## Picosecond Raman studies of dynamic charge localization following metal to ligand charge transfer excitation in tris (2,2'-bipyridyl) ruthenium (II)

Y. J. Chang, L. K. Orman, D. R. Anderson, T. Yabe, and J. B. Hopkins  
*Department of Chemistry, Louisiana State University, Baton Rouge, Louisiana 70803*

(Received 18 May 1987; accepted 30 June 1987)

In recent years there has been intense interest<sup>1,2</sup> in the photochemistry of metal complexes such as tris (2,2'-bipyridyl) ruthenium (II), hereafter written Ru(bpy)<sub>3</sub>. Current interest concerns the fate of the electron following photoinduced metal to ligand charge transfer. In particular, the important unanswered question is whether the electron is initially localized on a single bipyridyl ligand or delocalized over the three symmetry-equivalent ligands. In liquid solution there is strong experimental evidence that localization is complete on a nanosecond<sup>3-5</sup> and even picosecond<sup>6</sup> time scale. However, in the solid-state and low-temperature glasses it is thought that the electron is initially delocalized and evolves toward a localized configuration.<sup>7-9</sup>

We have studied these questions using picosecond resonance Raman spectroscopy. High-sensitivity Raman spectra were produced by a powerful, high repetition rate picosecond laser system pioneered in our laboratory.<sup>10</sup> The technique employs amplification and temporal compression of picosecond pulses in a regenerative amplifier at a repetition rate of 2 kHz.

We have observed the picosecond Raman spectrum of Ru(bpy)<sub>3</sub> in H<sub>2</sub>O as shown in Fig. 1(a). The spectra are consistent with previous nanosecond<sup>3-5</sup> and picosecond<sup>6</sup> re-

sults where all observed excited state bands have been assigned to the localized configuration. We have measured the dynamics of the Raman spectrum at pulse widths of 30, 80, and 150 ps at constant laser power. Only data at 150 ps are shown. If the delocalized state decays dynamically into a localized state on the time scale of the laser pulse, the Raman spectrum of Ru(bpy)<sub>2</sub>(bpy)<sup>-</sup> should increase with respect to Ru(bpy)<sub>3</sub> as the pulse width increases. No change in the relative intensities between Ru(bpy)<sub>2</sub>(bpy)<sup>-</sup> and Ru(bpy)<sub>3</sub> was observed as the laser pulse width was varied. We can therefore conclude that in H<sub>2</sub>O at 22 °C, charge localization is complete on a time scale fast compared to 30 ps.

We have investigated the possibility of solvent trapping of an initially delocalized electron by studying the dynamics of Ru(bpy)<sub>3</sub> MLCT states in high-viscosity fluid solution at 22 °C. Picosecond Raman spectra of Ru(bpy)<sub>3</sub> in H<sub>2</sub>O and glycerol are shown in Fig. 1 for laser pulse widths of 30 and 150 ps. Comparing the top H<sub>2</sub>O spectrum (a) with the glycerol spectrum (b), it is evident that the excited state bands associated with the localized MLCT states have become reduced in intensity. When the laser pulse width is changed from 150 ps as in Fig. 1(b) to 30 ps as in Fig. 1(c), the excited state localized MLCT bands diminish further. Clear-